



HAL
open science

Kriging and expected Improvement applied to an industrial context-Prediction of new geometries increasing the efficiency of fans

Agnès Lagnoux, T.M. Ngoc Nguyen, Bruno Demory, Manuel Henner

► To cite this version:

Agnès Lagnoux, T.M. Ngoc Nguyen, Bruno Demory, Manuel Henner. Kriging and expected Improvement applied to an industrial context-Prediction of new geometries increasing the efficiency of fans. 2021. hal-02044258v2

HAL Id: hal-02044258

<https://hal.science/hal-02044258v2>

Preprint submitted on 15 Jan 2021

HAL is a multi-disciplinary open access archive for the deposit and dissemination of scientific research documents, whether they are published or not. The documents may come from teaching and research institutions in France or abroad, or from public or private research centers.

L'archive ouverte pluridisciplinaire **HAL**, est destinée au dépôt et à la diffusion de documents scientifiques de niveau recherche, publiés ou non, émanant des établissements d'enseignement et de recherche français ou étrangers, des laboratoires publics ou privés.

Kriging and expected improvement combined to an industrial context - Prediction of new geometries increasing the efficiency of fans

Titre: Krigeage et amélioration attendue à visée industrielle - Prédiction de nouvelles géométries de systèmes de ventilation améliorant le rendement

Agnès Lagnoux¹, Thi Mong Ngoc Nguyen², Bruno Demory³ and Manuel Henner³

Abstract: This study has been done in cooperation with the automotive supplier Valeo. In automotive industry, client needs evolve quickly in a competitiveness context, particularly, regarding the fan involved in the engine cooling module. The practitioners are asked to propose “optimal” new fans in short times. Unfortunately, each evaluation of the underlying computer code may be expensive whence the need of approximated models and specific, parsimonious, and efficient global optimization strategies. In this paper, we propose to use the Kriging interpolation combined with the expected improvement algorithm to provide new fan designs with high performances in terms of efficiency. As far as we know, such a use of Kriging interpolation together with the expected improvement methodology is unique in an industrial context and provide really promising results.

Résumé : Cette étude résulte d’une collaboration avec Valeo, partenaire industriel. Dans l’industrie automobile, les besoins du marché évoluent très rapidement dans un contexte où la concurrence est forte et tout particulièrement concernant les systèmes de ventilation qui jouent un rôle clef dans le système de refroidissement du moteur. Les ingénieurs doivent dans ce contexte proposer des géométries de pales “optimales” dans des délais très courts. Malheureusement, les codes numériques sont coûteux à évaluer et des méthodes d’approximations et des techniques d’optimisation spécifiques doivent être développées. Nous proposons de combiner l’interpolation par krigeage et l’algorithme d’optimisation d’amélioration attendue pour déterminer des géométries de pales ayant de bonnes performances en termes de rendement. Une telle application industrielle basée sur le krigeage et l’amélioration attendue semble inédite et fournit d’excellents résultats.

Keywords: Kriging, expected improvement, optimization

Mots-clés : Krigeage, amélioration attendue, optimisation

AMS 2000 subject classifications: 35L05, 35L70

1. Introduction and Motivations

Many mathematical models encountered in applied sciences involve a computer code (also called a “black-box” simulator) given by an unknown deterministic real-valued function $f: D \subset \mathbb{R}^d \rightarrow$

¹ Institut de Mathématiques de Toulouse; UMR5219. Université de Toulouse; CNRS. UT2J, F-31058 Toulouse, France.

E-mail: lagnoux@univ-tlse2.fr

² Faculty of Mathematics & Computer Science, University of Science, VNU-HCMC, Ho Chi Minh City, Viet Nam. Vietnam National University, Ho Chi Minh City, Viet Nam.

E-mail: ngtmngoc@hcmus.edu.vn

³ Valeo, 8, rue Louis Lormand CS 80517 La Verrière, France.

E-mail: bruno.demory@valeo.com; manuel.henner@valeo.com

\mathbb{R} defining an input/output relation. In several engineering problems, the goal is then to optimize the function f . In practice, the number of function evaluations may be severely limited by time or cost and the practitioners typically dispose of a very limited evaluation budget. Consequently, the computational time required for each evaluation of the computer code together with the possibly high dimension of the input space generally do not allow an exhaustive exploration of the input space under realistic industrial time constraints. Moreover, in most cases, the non-availability of derivatives prevents one from using gradient-based techniques. Similarly, the use of metaheuristics (e.g., genetic algorithms) is compromised by severely limited evaluation budgets. Hence, such limitations pose a serious challenge to the field of global optimization and statistical approaches are mandatory to propose surrogate models and to search optima in reasonable short time.

A first step in that direction consists in proposing mathematical approximations of the input/output relation, namely “metamodels” or “surrogate models”. These response surfaces can then be used for visualization, prediction, and optimization. Their construction relies on a prior knowledge consisting in available observations (data collected by evaluating the objective function f at a few points) provided by the practitioner. More precisely, the user dispose of a sample of N observations $f(x_1), \dots, f(x_N)$ at locations x_1, \dots, x_N to realize inference and to construct an accurate metamodel. In such a framework, it is worth noticing that the uncertainty does not refer to a random phenomenon but to a partially observed deterministic one. Due to the limited evaluations budget, the need to select cautiously evaluation points when attempting to solve this problem appears to be crucial. Several strategies have been developed like moving average (Ripley, 1981, p.36), linear regression (Ripley, 1981, p.29), splines (Cressie, 1993, p.181), Kriging interpolation Stein (1999); Rasmussen and Williams (2006), bayesian strategies Gaudard et al. (1999), neural networks Bryan and Adams (2002)... See also Arnaud and Emery (2000); Bailargeon (2005) for a more complete review. In this paper, we consider the Kriging interpolation as metamodel. In Kriging, the unknown computer code f that is to be estimated is assumed to be the realization of a Gaussian process. The exploitation of a N sample $f(x_1), \dots, f(x_N)$ of observations at locations x_1, \dots, x_N allows working on the conditioned process which is known to be Gaussian at any point with known mean and known variance. This conditional Gaussianity, together with the explicit expressions of the conditional moments, is one of the main reasons why Gaussian processes and Kriging are attractive and have become so popular during the last decades.

The second step wants to make use of the Kriging interpolation to proceed to the global optimization (say, maximization). The key to using response surfaces for global optimization lies in balancing the need to exploit the approximating surface (by sampling where it is maximized) with the need to improve the approximation (by sampling where prediction error may be high). Proceeding to the direct optimization of the Kriging mean then appears to be appealing. Nevertheless, optimizing directly a deterministic metamodel (like the Kriging mean, or even a spline or a polynomial) may be inefficient and may lead to artificial optima, as shown numerically in Jones (2001). Fortunately, several efficient criteria have been introduced to tackle such a problem, like expected improvement, knowledge gradient,... Jones et al. (1998). By its nice properties and its analytical tractability, expected improvement has become one of the most attractive procedure. Its principle is simple and natural: it measures the improvement brought by a point in the maximization of the function f and then chooses new points that maximizes the improvement. A

balance is then made between the exploration of regions where prediction error may be high and the exploitation of promising regions that would yield a notably improvement.

This paper is the result of a fruitful cooperation between academic researchers of the Institut de Mathématiques de Toulouse and Valeo, an industrial partner. It has been realized during the project PEPITO supported by the French National Research Agency (ANR). Aims were to experiment an extreme approach based on intensive and multiphysical simulations, the use of parametrized geometries, the determination of designs of experiments with large number of factors and the search for optima in large and high dimensional domains. In particular, we were interested in the fan involved in the engine cooling module that plays a key role in the engine durability and remains an important focus of the engineering teams. The practitioners are asked to propose in short time new fan designs answering the client requirements in terms of efficiency, torque, acoustics, packaging... Unfortunately, each evaluation of the computer code is time-consuming (about 3000 CPU.hour) and such a goal costly to achieve. In that view, we combined the use of the Kriging interpolation and the expected improvement algorithm to determine new “optimal” fan designs (with high performances). As far as we know, such an use of Kriging together with expected improvement is unprecedented in an industrial context and provide really promising results.

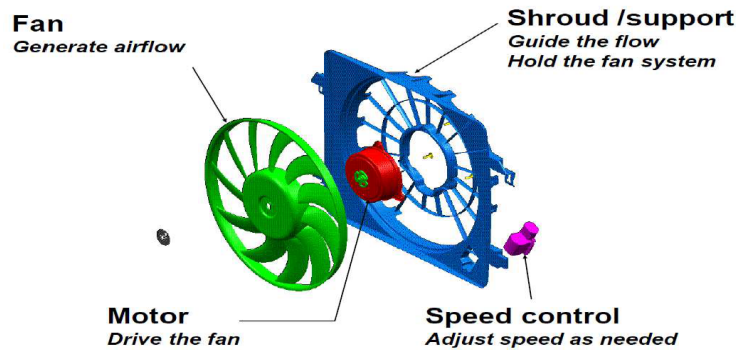
The paper is organized as follows. In Section 2, we present the industrial context together with the description of the input and output variables involved in the computer code. Sections 3 and 4 are devoted to the presentation of the Kriging interpolation and the expected improvement optimization algorithm. The numerical results are presented in Section 5. Finally, Section 6 concludes this article.

2. The industrial context

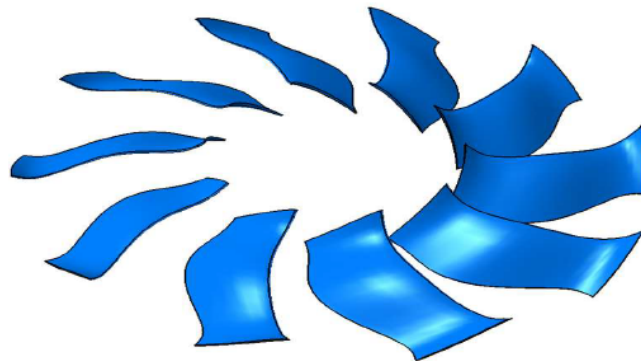
Due to the ever changing geometry and architecture of cars, original equipment makers are constantly requesting new fans that perfectly fit to their needs. The specifications are given most of the time by the performances at a *design point* (pressure and maximum efficiency are targeted), an *off-design condition* (lower pressure but higher flow rate), and an acoustic level for the nominal point (fan noise is mostly perceptible at vehicle idle). Electrical consumption and packaging are of course part of the equation, and the resulting design must be seen as a compromise between different objectives.

The study presented in this paper focuses particularly on the optimization of the fan blade. A representation of a typical fan system architecture is presented in Figure 1. It shows a complex system which design requires a good expertise in both fields of turbomachine and automotive integration.

Recent developments have been greatly accelerated with the use of numerical simulation, which has allowed engineers to reduce the number of prototypes and the test campaigns. The main difficulty lies in the increased complexity which is due to the antagonist criteria of higher performance requirements and reduced space in engine compartment. In addition, the time allocated by the manufacturers to answer to any new specification with a new development is drastically reduced. In this context, the lead time of the simulation and the amount of data produced are not necessarily compatible with the multiple iterations required. Fortunately, recent advances in simulation (both hardware and software) make its use more affordable and allow the

FIGURE 1. *Fan system architecture*

practitioner to run automated calculations daily instead of using much human time of an expert engineer. Such an opportunity opens the door to optimization processes that use simulation intensively. Interesting results have already been found as demonstrated in Figure 2, with blade shapes that are innovative and non-intuitive for the expert knowledge.

FIGURE 2. *Innovative blade shape: not intuitive, not given by current theory*

In the next two subsections, we describe properly the computer code leading to the selected responses and the industrial problem.

2.1. *Description of the computer code*

The physical phenomena yielding the industrial responses like the pressure rise (downstream pressure minus upstream pressure), the torque (integral of moments due to pressure and viscous forces), the global efficiency of the fan and other local variables on both rotor and stator, acoustics, mass, size,... are complex. Mathematically, they are represented by an input/output relation,

called the black-box model, given by

$$f: \mathbb{R}^d \times [0, \infty) \rightarrow \mathbb{R}^p \\ (x_1, \dots, x_d, Q) \mapsto (y_1, \dots, y_p) = f(x_1, \dots, x_d, Q).$$

In our study, the selected responses are the pressure rise (ΔP in Pa), the torque (C in N.m), and the global efficiency (R in %) of the fan so that $p = 3$. One may notice that the fan efficiency R is directly related to the two other global variables ΔP and C by the following relation

$$R = \frac{Q \times \Delta P}{C \times \Omega},$$

Q being the flow rate (m³/s) and Ω the rotational speed (rad⁻¹). In practice, the practitioner expects a static efficiency of about 55%.

The input factors x_1, \dots, x_d involved in the computer code f are related to the full cooling module and in particular to the fan parametrization. The fan is composed of several blades which are equivalent to rotating wings. The blade section at a constant radius is an aerodynamic profile with characteristics of lift and drag, which create respectively the pressure rise and the torque of the fan. Some of the fan parameters are represented in Figure 3 and some others specific to the blade can be found in Figure 4. Using a satisfactory number of factors would lead to select 60 of them for the cooling module. Anyway, in order to make things feasible, only 14 parameters have been highlighted via a preliminary sensitivity analysis based on Sobol indices and thanks to the expert knowledge (see [Moreau et al. \(2004\)](#); [Grondin et al. \(2005\)](#)), while the others are fixed to their nominal values. Twelve geometrical factors (sweep (2), max camber height (2), stagger angle (4), chord length (4)) are selected, and two others are added to size a plate behind the fan in order to represent the aerodynamic blockage due to the thermal engine of the car (it is placed behind the fan and acts as an obstacle similarly to the flow in the underhood). The flow rate is the physical factor giving the 15th parameter. Hence $d = 14$.

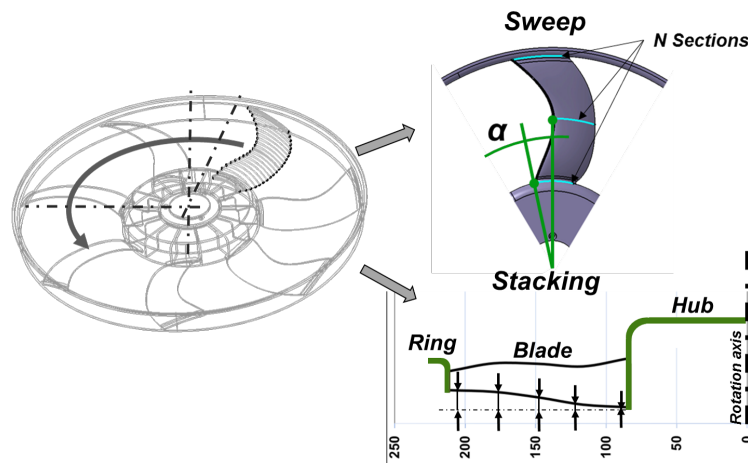
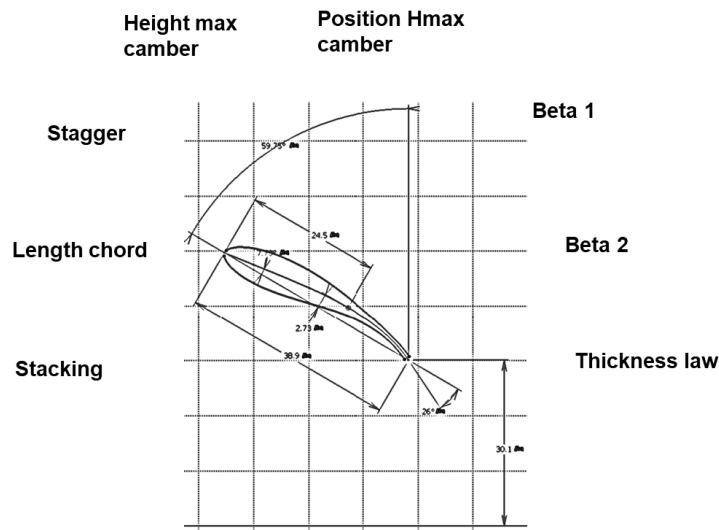


FIGURE 3. *Fan description*

FIGURE 4. *Profile parameters*

2.2. The industrial problem

In this study, the focus is made on innovative fan designs that will improve the fan efficiency and we want to propose an enhanced optimization method able to handle enough parameters for the design of the most efficient, quiet and compact fans in a short time frame.

As mentioned in the introduction, direct optimization, which is based on a gradient descent algorithm, is a fairly common solution. However, it has the drawbacks of producing only local optima, and therefore of having to be repeated for each new optimization with lengthy calculation iterations. It should also be mentioned that the case of multi-objective optimization requires the creation of a cost function which sets the trade-off between the different objectives, and does not produce a Pareto front that could be analyzed by engineers. On the other hand, the exhaustive search for an optimum is made very difficult by the large number of parameters, which moreover have interactions between them. Exploration in a field of dimension 14 greatly exceeds the capabilities of an engineer, as expert as he could be in turbomachine field. Such an exploration is also intractable statistically speaking. Last but not least, each evaluation of the output is a time-consuming with traditional iterative processes and costly task. In such a context, a proper strategy for the optimization process both efficient and parsimonious is required.

In this paper, we chose the Kriging interpolation to construct a surrogate model easy and cheap to evaluate. Then we combine it to the so-called expected improvement optimization algorithm to build efficient new fan designs. In the next two sections, we present the Kriging interpolation also used in the sequel together with the expected improvement methodology and the description of of the numerical application and with its results are presented in Section 5.

3. Kriging

Originally introduced in geosciences by [Krige \(1951\)](#), Kriging is a stochastic method of interpolation. The aim is to predict the value of a natural phenomenon at any arbitrary location of interest from the measured observations at the sample points. The theoretical basis was first developed in the 1960's by [Matheron \(1962, 1963\)](#). See also the famous and well-documented references on the topic [Stein \(1999\)](#); [Santner et al. \(2003\)](#); [Rasmussen and Williams \(2006\)](#). Nowadays, Kriging is widely used in the domain of spatial analysis and computer experiments. From a mathematical point of view, we consider a function $f: x \in D \subset \mathbb{R}^d \mapsto f(x) \in \mathbb{R}$ and we wish to predict $f(x_0)$ from a sample of N observations $(f(x_1), \dots, f(x_N))$ at locations x_1, \dots, x_N . The key ingredient of Kriging is that f is assumed to be a realization of a process $Y: D \subset \mathbb{R}^d \rightarrow \mathbb{R}$ with mean function $m: x \in \mathbb{R}^d \mapsto m(x) \in \mathbb{R}$ and covariance kernel $k: (x, y) \in \mathbb{R}^d \times \mathbb{R}^d \mapsto k(x, y) \in \mathbb{R}$. Then, Kriging uses a weighted average of the observations as estimate. The weights are chosen so that the Kriging prediction is unbiased with minimal variance error.

In order to illustrate Kriging, we develop the methodology in the particular setting of what is called the *simple Kriging* in which the process Y is assumed to be centered and stationary at order 2 with known covariance function k . Let the vector $r_N(x_0)$ be given by

$$r_N(x_0) = (\text{Cov}(Y(x_0), Y(x_1)), \dots, \text{Cov}(Y(x_0), Y(x_N)))^\top = (k(x_0, x_1), \dots, k(x_0, x_N))^\top$$

and the square matrix R_N of the covariances on the observation points of size $N \times N$ given by

$$R_N = \begin{pmatrix} \text{Cov}(Y(x_1), Y(x_1)) & \dots & \text{Cov}(Y(x_1), Y(x_N)) \\ \vdots & \dots & \vdots \\ \text{Cov}(Y(x_N), Y(x_1)) & \dots & \text{Cov}(Y(x_N), Y(x_N)) \end{pmatrix} = \begin{pmatrix} k(x_1, x_1) & \dots & k(x_1, x_N) \\ \vdots & \dots & \vdots \\ k(x_N, x_1) & \dots & k(x_N, x_N) \end{pmatrix}.$$

Then the (random) Kriging prediction writes

$$\hat{Y}(x_0) = \sum_{i=1}^N \lambda_i^*(x_0) Y(x_i), \quad (1)$$

where the optimal vector

$$\lambda^*(x_0) = (\lambda_1^*(x_0), \dots, \lambda_N^*(x_0))^\top = R_N^{-1} r_N(x_0)$$

is obtained by minimizing the quadratic error.

One of the main interest of Kriging is that the Kriging variance is explicitly known:

$$\sigma_N^2(x_0) = \mathbb{E} \left[(Y(x_0) - \hat{Y}(x_0))^2 \right] = k(x_0, x_0) - r_N^\top(x_0) R_N^{-1} r_N(x_0), \quad (2)$$

allowing the practitioner to build confidence intervals. Furthermore, if the underlying process Y is Gaussian and observed at a given N -uplet $(y_1, \dots, y_N)^\top$, we have the much stronger result that the conditional distribution of $Y(x_0)$ given $(Y(x_1), \dots, Y(x_N)) = (y_1, \dots, y_N)$ is Gaussian with mean $\sum_{i=1}^N \lambda_i^*(x_0) y_i$ and variance $\sigma_N^2(x_0)$ so that the Kriging prediction is the best predictor (in terms of minimizing the variance of the prediction error), linear or non linear ([Rice, 2006](#), p.140).

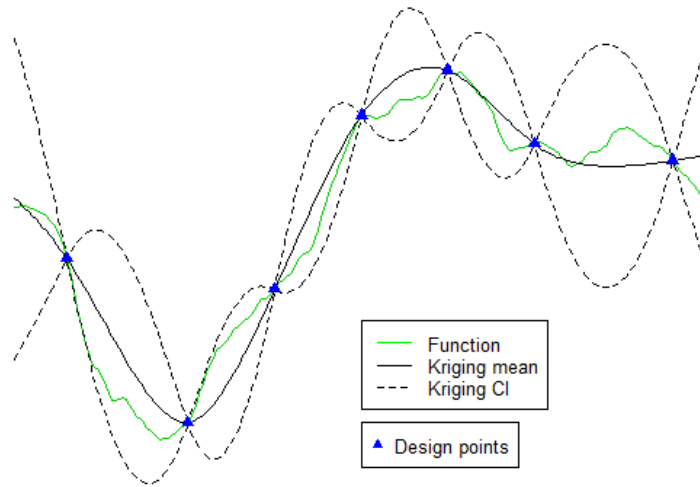


FIGURE 5. Example of one-dimensional data interpolation by Kriging, with confidence intervals. The green curve shows the function f . Triangles in blue indicate the location of the data. The Kriging interpolation, shown in black, runs along the means of the normally distributed confidence intervals shown in dashed lines.

Notice that if covariance parameters are unknown, several estimation procedures exist; then the estimated covariance parameters are plugged in (1) and (2). For instance, the unknown parameters can be estimated by maximum likelihood. As proposed in the function “km” of the R package `DiceKriging` that performs Kriging, penalized maximum likelihood estimation is also possible if some penalty is given, or Leave-One-Out for noise-free observations.

Figure 5 represents the Kriging interpolation on a toy example. In this example, the unknown function f is represented by the green curve. The practitioner provides an initial design consisting in 7 points y_1, \dots, y_7 observed at x_1, \dots, x_7 and represented by blue triangles. The Kriging interpolation is represented by the black curve. The dashed curves represent the Kriging confidence intervals.

4. Expected improvement

The goal is to optimize a function $f: D \subset \mathbb{R}^d \rightarrow \mathbb{R}$. As explained in the introduction, it would be tempting to replace the costly simulator f by the Kriging interpolation and to directly optimize it. Anyway, such a procedure is generally not efficient as demonstrated numerically in Jones (2001). Furthermore, it may potentially lead to artificial optima in case of iterated optimizations with metamodel update. Fortunately, efficient criteria like the expected improvement have been proposed for sequential Kriging-based optimization (see, e.g., for a comparative criteria study Schonlau (1997) and Sasena et al. (2002)).

In this section, we present briefly the expected improvement optimization algorithm, first introduced by Mockus Moćkus (1975) and further combined with the Gaussian processes model in the efficient global optimization (EGO), see e.g. Jones et al. (1998), and sequential Kriging

optimization (SKO), see e.g. [Huang et al. \(2006\)](#). These two methods are the key ingredient for most Bayesian optimization algorithms. The reader may follow the references therein for more details.

Presentation of the algorithm In view of maximizing the function f , we aim at proposing a point x^* so that $f(x^*)$ is as close as possible to $\max_{x \in D} f(x)$. Similarly to Kriging, we consider that f is a realization of a Gaussian process Y with known mean function m and covariance kernel k . The point x^* is derived as the best point from the sample pairs $\{(x_1, f(x_1)), \dots, (x_N, f(x_N))\}$. The points x_1, \dots, x_N are chosen repeatedly following a three steps procedure.

Step 1 - Initial design. For N such that $(N < N_s)$ (e.g. $N = N_s/2$), we choose the points x_1, \dots, x_N using a space filling criterion. For instance, one may use a latin hypercube sampling (LHS) [Jin et al. \(2005\)](#) or an orthogonal array (OA) [Owen \(1992\)](#). Then we evaluate $f(x_1), \dots, f(x_N)$.

Step 2 - Sequential incrementation. For $n = N, \dots, N_s - 1$, we derive x_{n+1} from the current sample pairs $\{(x_1, f(x_1)), \dots, (x_n, f(x_n))\}$ using the distribution of Y conditioned on $\{Y(x_1) = f(x_1), \dots, Y(x_n) = f(x_n)\}$. More precisely, the next point x_{n+1}^{EI} is chosen such that

$$x_{n+1} \in \operatorname{argmax}_{x \in D} \mathbb{E} \left[(Y(x) - \max\{f(x_1), \dots, f(x_n)\})^+ \mid Y(x_1) = f(x_1), \dots, Y(x_n) = f(x_n) \right]$$

where $(\cdot)^+$ stands for the positive part, namely $\max\{\cdot, 0\}$. Let us denote by $EI_n(x)$ the *Expected Improvement* given by

$$EI_n(x) = \mathbb{E} \left[(Y(x) - \max\{f(x_1), \dots, f(x_n)\})^+ \mid Y(x_1) = f(x_1), \dots, Y(x_n) = f(x_n) \right].$$

Finally, we evaluate $f(x_{n+1})$.

Then one can proceed to the final step.

Step 3 - Proposition of a new design point. The solution is the point x^* such that

$$x^* = \operatorname{argmax}_{x \in \{x_1, \dots, x_{N_s}\}} f(x).$$

Expected improvement properties The principle of the expected improvement procedure is simple and natural: it measures the improvement brought by a point x in the maximization of the function f and then chooses new points that maximizes the improvement.

The criterion EI_n has nice properties: first, it is strictly positive as soon as the Kriging variance is, second, it cancels if the Kriging variance is zero and the Kriging mean is smaller than the actual maximum given by $M_n = \max\{f(x_1), \dots, f(x_n)\}$ and finally, it increases with the Kriging mean. Moreover, $EI_n(x)$ has an explicit expression given by

$$EI_n(x) = (\hat{Y}(x) - M_n) \Phi \left(\frac{\hat{Y}(x) - M_n}{\sigma_n(x)} \right) + \sigma_n(x) \phi \left(\frac{\hat{Y}(x) - M_n}{\sigma_n(x)} \right)$$

where ϕ and Φ are respectively the probability density function and the cumulative distribution function of the standard Gaussian law and $\hat{Y}(x)$ and $\sigma_n^2(x)$ are respectively the Kriging mean and

the Kriging variance after n measurements. See (1) and (2) in Section 3 for their expressions. Consequently, one may calculate exactly $EI_n(x)$ in $O(n^2)$. More precisely, once the inversion of R_n has been done (with a computational cost in $O(n^3)$) and stored, each evaluation $EI_n(x)$ of the expected improvement criterion is in $O(n^2)$ due to the computation of the quadratic form $r_n(x)^\top R_n^{-1} r_n(x)$ involved in the conditional variance $\sigma_n^2(x)$ (see (2) in Section 3). Convergence guarantees for the expected improvement algorithm are given in [Vazquez and Bect \(2010\)](#); [Bect et al. \(2018\)](#).

Another methodologies for choosing x_{n+1} have been developed like knowledge gradient that is a close variant of the expected improvement algorithm [Frazier et al. \(2008\)](#); [Scott et al. \(2011\)](#). Anyway, the exact computation of the knowledge gradient function being more costly than expected improvement, practitioners prefer to use the expected improvement algorithm.

Figure 6 represents the expected improvement algorithm on a toy example. In this example, the unknown real code is represented by the green curve. The practitioner provides an initial design consisting in 7 points represented by blue triangles. First, we proceed to the Kriging interpolation leading to the black curve. The dashed curves represent the confidence intervals of the Kriging interpolation. Second, we proceed to the computation of the expected improvement criterion. Finally, the new point to predict is chosen in the most promising region: with highest value of expected improvement.

Parallelizations: expected improvement multi-points Now, the goal is to propose several new points at each iteration of the algorithm. In that view, the second step of the sequential incrementation is updated in the following way.

New step 2 - Sequential incrementation by batch Let $b \in \mathbb{N}^*$ be the size of the batch, namely the number of new points to be proposed at each iteration. For $n = N, \dots, N_s - 1$, we derive $x_{n+1,1}, \dots, x_{n+1,b}$ from the current sample pairs

$$\{(x_1, f(x_1)), \dots, (x_N, f(x_N)), (x_{N+1,1}, f(x_{N+1,1})), \dots, (x_{N+1,b}, f(x_{N+1,b})), \dots, (x_{n,b}, f(x_{n,b}))\}$$

and using the distribution of Y conditioned on $\{Y(x_1) = f(x_1), \dots, Y(x_k) = f(x_k), Y(x_{k+1,1}) = f(x_{k+1,1}), \dots, Y(x_{k+1,b}) = f(x_{k+1,b}), \dots, Y(x_{n,b}) = f(x_{n,b})\}$. To shorten notation, we still denote the observation vector y . We also introduce the current maximum:

$$M_n = \max\{f(x_1), \dots, f(x_k), f(x_{k+1,1}), \dots, f(x_{k+1,b}), \dots, f(x_{n,b})\}.$$

Now the expected improvement criterion rewrites as:

$$(x_{n+1,1}, \dots, x_{n+1,b}) \in \operatorname{argmax}_{(x'_1, \dots, x'_b) \in D^b} \mathbb{E} \left[(\max\{Y(x'_1), \dots, Y(x'_b)\} - M_n)^+ | y \right].$$

The quantity to optimize in the right-hand side of the previous equation is naturally denoted by $EI_n(x'_1, \dots, x'_b)$. Unlike in the case of a single new point at each iteration, the evaluation of $EI_n(x'_1, \dots, x'_b)$ is now complex. In [Chevalier and Ginsbourger \(2013\)](#), the authors proposed different strategies to compute it.

First, one may use a Monte Carlo scheme noticing that $EI_n(x'_1, \dots, x'_b)$ is the expectation of the function of a Gaussian vector with a known distribution.

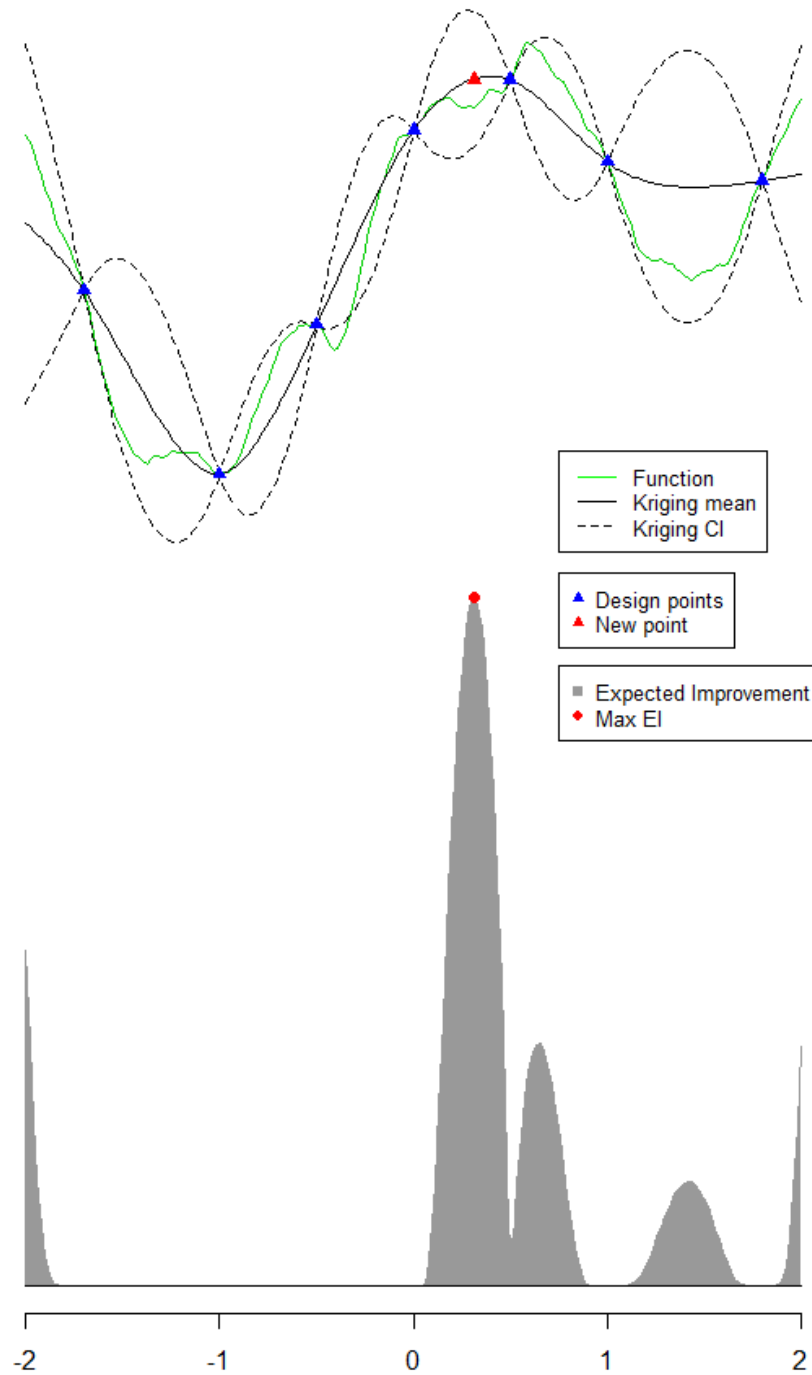


FIGURE 6. *Illustration of the expected improvement algorithm applied to Kriging*

Second, the heuristic Constant Liar (CL) method may also be used [Ginsbourger et al. \(2008\)](#); [Chevalier and Ginsbourger \(2013\)](#). To begin, the regular expected improvement is maximized. Then, for the next points, the expected improvement is maximized again, but with an artificially updated Kriging model. Since the response values corresponding to the last best point obtained are not available, the idea of CL is to replace them by an arbitrary constant value (the "lie") set by the user. We proceed repeatedly so that the trick relies in the fact that only single point expected improvement need to be evaluated. More precisely, for any $i = 1, \dots, b$, we assume that $Y(x_{n+1,1}) = \tilde{y}_1, \dots, Y(x_{n+1,i-1}) = \tilde{y}_{i-1}$, we set

$$x_{n+1,i} \in \operatorname{argmax}_{x \in D} \mathbb{E} \left[(Y(x) - \max\{f(x_1), \dots, f(x_n, b), \tilde{y}_1, \dots, \tilde{y}_{i-1}\})^+ | y \right],$$

we introduce a value \tilde{y}_i , and so on. The values $\tilde{y}_1, \dots, \tilde{y}_{b-1}$ can be chosen as the maximum of all the observed values of f so that the expected improvement algorithm tends to explore the function near the current maximum (as the lie is a high value and we are maximizing f). Besides, taking the minimum of all the observed values of f leads to a more exploratory expected improvement procedure. Naturally, considering the current maximum (respectively minimum) is expected to perform well on unimodal (resp. multimodal). Alternatively, one may use the Kriging mean as liars or even mix strategies taking both the current minimum and the current maximum. Then, at each iteration, two batches are generated with both strategies. From these two candidate batches, the batch with the best actual expected improvement value is chosen.

Third, one may compute exactly $EI_n(x'_1, \dots, x'_b)$ via b^2 evaluations of multidimensional Gaussian cumulative distribution functions.

Extension to multi-objectives Similarly to co-Kriging, the expected improvement algorithm can be generalized to optimize a multivariate function $f = (f_1, \dots, f_p)$ from $D \subset \mathbb{R}^d$ to \mathbb{R}^p . In that view, the several objectives f_1, \dots, f_p are considered as realizations of p Gaussian processes Y_1, \dots, Y_p . The conditional expectation now represents the expectation conditioned on all the observed values $\{f_1(x_1), \dots, f_1(x_n), f_2(x_1), \dots, f_p(x_n)\}$. The optimization is seen as a sequential reduction of the volume of the excursion sets below the current best solutions and the strategy chooses the points that give the highest expected reduction. The reader may refer to [Picheny \(2015\)](#) for the details of such a generalization.

5. Prediction of new geometries

5.1. Available data and software

An automated simulation process has been implemented to drive design of experiment plans, using several softwares that are commonly used in the industry. At first, the design of the fan system has been completely parameterized in a computer-aided design (CAD) tool named *Catia*³, according to rules that allow all combinations of geometric parameters in their possible ranges of variation, while ensuring their independence. CAD files are exported in a standard format and re-read by a fluid simulation software (StarCCM+), which provides by scripts automated

³ <https://www.3ds.com/products-services/catia/>

meshes, model solving and automatic post-processing of results. A third tool used for optimization (Isight⁴) ensures the sequence of tasks by imposing the set of parameters and launching CAD and simulation tools. The different sets of data are given by Latin hypercube sampling (LHS) plans (see, e.g. Jin et al. (2005) for an introduction to LHS) produced by Isight or by factorial plans⁵.

Once the quality of the simulations is proved and the results are obtained for the various plans, some initial meta-models have been produced by neural networks (Isight, Radial basis function models) and their accuracies checked by comparing the prediction (neural network) and the real experiment (simulation). Some good results were observed, and in general the trends are correctly predicted when moving one parameter. However the accuracy of the model is questionable since the number of runs is still very low compared to the size of the domain. Large errors are frequently observed which justifies some additional effort towards the implementation of a good optimization process which is the goal of this paper.

Concretely, Valeo engineers provide us a design of experiment together with the corresponding selected responses in order to lead our statistical study. More precisely, they supply a design of experiment of 300 geometries in \mathbb{R}^{14} using the OLHS procedure. For any geometry, they compute the pressure rise ΔP , the torque C and the efficiency R at a flow rate $Q = Q_{\text{DoE}}$ whose value runs between 1000 and 4000. It must be noted that the physical factor for the flow rate Q has been set to Q_{DoE} according to the plan, and that the simulations were done additionally twice for the two different flow rates $Q_{\text{low}} = 1000$ and $Q_{\text{high}} = 4000$. In addition, they provide 600 geometries in \mathbb{R}^{14} also constructed via OLHS and the values of $(\Delta P, C, R)$ for any geometry at two different flow rates Q : Q_{DoE} and $Q_{\text{high}} = 4000$. In this paper, we focus on the efficiency only.

The numerical experiments are implemented using the R packages `DiceKriging` and `DiceOptim` to perform respectively Kriging and expected improvement (see Roustant et al. (2012)).

5.2. Preliminary study and selection of the Kriging interpolation

A preliminary study has been led to compare different strategies to model the data. First, we considered a linear regression model on the efficiency R given by:

$$R_{\text{lin}}(g; Q) = \beta_0 + \sum_{j=1}^{14} \beta_j g_j + \beta_{15} Q + \varepsilon$$

where the β_j 's are unknown coefficients, $g = (g_j)_{j=1, \dots, 14}$ is the input multivariate variable, namely the geometry, Q is the flow rate considered and ε is a white noise. The second model considered was given by:

$$R_{\text{approx}}(g; Q) = \alpha_0 + \sum_{j=1}^{14} f_j(g_j) + f_{15}(Q) + \varepsilon$$

⁴ <https://www.3ds.com/products-services/simulia/products/isight-simulia-execution-engine/latest-release/>

⁵ A great care was given to the simulation convergence, all runs being maintained until monitored performances were stabilized and residuals went below strict criteria. In addition, some runs were repeated on different machines or with different rules of parallelization to check that no discrepancy appears in the process.

where α_0 is an unknown constant, $(f_j)_{j=1,\dots,15}$ are deterministic approximation functions (e.g. natural cubic splines) and ε is a white noise. Several simulations showed that Kriging outperforms the latter two models in terms of precision.

5.3. Experiment description

As explained previously, the aim is to propose several fan designs leading to good performances in terms of efficiency. In that view, we exploit the two designs of experiment provided by Valeo and presented in Section 5.1. Then we combine Kriging and expected improvement to achieve this goal.

Kriging and expected improvement on the efficiency R at $Q_{\text{high}} = 4000 \text{ m}^3/h$ In this section, we consider all the available information gathering the data available corresponding to a flow rate Q_{high} equal to $4000 \text{ m}^3/h$. Namely, we consider the 900 different geometries of the two designs of experiment provided by Valeo and their corresponding efficiencies at $4000 \text{ m}^3/h$. Then, we first perform simple Kriging on these efficiencies using the function “km” of the R package `DiceKriging`. In other words, as explained in Section 3, we consider that the efficiency R at $Q_{\text{high}} = 4000 \text{ m}^3/h$ is the realization of a Gaussian process with unknown mean μ and covariance function k :

$$R(g; 4000) = \mu(4000) + \varepsilon(g; 4000)$$

for any geometry g living in \mathbb{R}^{14} . In the sequel, we assume that ε is a centered homoscedastic Gaussian process with variance σ^2 . In addition, we use a separable covariance function k :

$$k(g, g') = \text{Cov}(\varepsilon(g; 4000), \varepsilon(g'; 4000)) = \sigma^2 \prod_{j=1}^{14} \rho_{\theta_j}(|g_j - g'_j|)$$

where the ρ_{θ_j} 's are unidimensional Matérn kernels with parameter $5/2$:

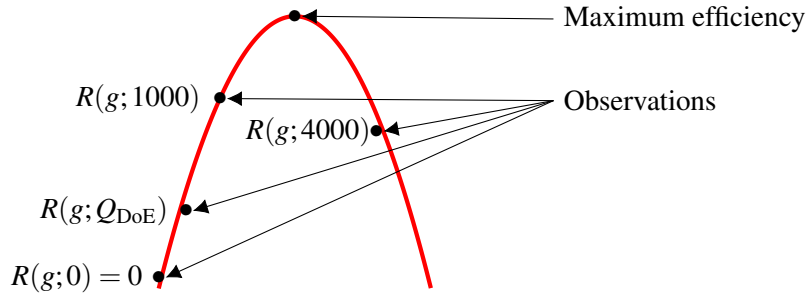
$$\rho_{\theta_j}(d) = \left(1 + \frac{\sqrt{5}d}{\theta_j} + \frac{5d^2}{3\theta_j^2} \right) \exp\left(-\frac{\sqrt{5}d}{\theta_j} \right).$$

The Matérn kernel has been preferred to the Gaussian kernel or to the exponential kernel since it corresponds to a trade-off between the latter two. Notice that the value of the correlation length θ_j which is unknown has great influence on the results: then it is of crucial importance. Hence, all the unknown parameters θ_j , for $j = 1, \dots, 14$ have been estimated automatically by the algorithm (data-driven algorithm) using maximum likelihood estimation, so do the two others unknown parameters, namely the unknown mean μ and the unknown variance σ^2 of the underlying Gaussian process.

Second, in order to maximize the efficiency at a flow rate Q equal to $4000 \text{ m}^3/h$, we run the expected improvement algorithm using the function “max_qEI” of the R package `DiceOptim` providing a batch of $n = 10$ new promising geometries. The optimization is realized with a multistarted brute force qEI maximization with Broyden-Fletcher-Goldfarb-Shanno (BFGS) algorithm that is an iterative method for solving unconstrained nonlinear optimization problems. The BFGS method belongs to quasi-Newton methods that seek a stationary point. See [Fletcher \(1987\)](#) for more details on the BFGS algorithm.

Kriging and expected improvement on the estimated efficiency at $Q = 2500$ Here, alternatively, we aim at working at a nominal flow rate of $2500 \text{ m}^3/\text{h}$ rather than at the maximum flow rate of $4000 \text{ m}^3/\text{h}$ previously considered. Unfortunately, the data at $Q = 2500 \text{ m}^3/\text{h}$ are not available. Instead, in the first design of experiment of size 300, Valeo supplied us three efficiencies R_{DoE} , R_{low} and R_{high} associated to 300 geometries at flow rates Q_{DoE} (whose value runs between $Q_{\text{low}} = 1000 \text{ m}^3/\text{h}$ and $Q_{\text{high}} = 4000 \text{ m}^3/\text{h}$), $Q_{\text{low}} = 1000 \text{ m}^3/\text{h}$ and $Q_{\text{high}} = 4000 \text{ m}^3/\text{h}$, respectively. Guided by the expert knowledge, we realize a quadratic regression on these efficiencies leading to one quadratic curve per geometry. More precisely, for any fixed geometry, we assume that $Q \mapsto R(g; Q)$ is a quadratic function of Q and we proceed to an interpolation of the efficiency using the efficiency values at $Q_0 = 0$, $Q_{\text{low}} = 1000 \text{ m}^3/\text{h}$, Q_{DoE} and $Q_{\text{high}} = 4000 \text{ m}^3/\text{h}$ of the 300 configurations of geometrical input parameters. Hence, at a fixed geometry g , the function $R(g; \cdot)$ is approximated by the quadratic function $\tilde{R}(g; \cdot)$ given by

$$\tilde{R}(g; Q) = a(g) \cdot Q^2 + b(g) \cdot Q + c(g).$$



Then, we compute the estimated efficiency \tilde{R} at $Q = 2500 \text{ m}^3/\text{h}$ of the 300 geometries of the design of experiment: $\tilde{R}(g; 2500) = a(g) \cdot (2500)^2 + b(g) \cdot 2500 + c(g)$. Finally, we perform Kriging on these estimated efficiencies $\tilde{R}(g; 2500)$ at $Q = 2500 \text{ m}^3/\text{h}$ and we run the expected improvement optimization algorithm to provide a batch of 10 promising fan geometries. We follow the procedure and choices of the previous paragraph.

Remark. Observe that we could have proceeded in a slightly different way to estimate the efficiencies at $Q = 2500 \text{ m}^3/\text{h}$ by performing a Kriging interpolation of the efficiency R in \mathbb{R}^{15} , considering the flow rate as an input parameter that may vary rather than working in \mathbb{R}^{14} with fixed flow rate.

Figure 7 synthesizes the different steps of the procedure adopted in this article. The gray boxes represent the directions for future work: adding linear functions in the Kriging means to improve the optimization step, comparing the upper confidence bound (UCB) optimization procedure to expected improvement, and consider the whole vector $(\Delta P, C, R)$ of outputs and perform co-Kriging and multi-objective expected improvement. When working at $Q = 4000 \text{ m}^3/\text{h}$, a similar diagram could be drawn skipping the quadratic interpolation step. See, for instance, Auer et al. (2002) for the description of the UCB optimization methodology and Srinivas et al. (2012) for the theoretical asymptotic properties of this algorithm.

Notation The Kriging means provided by the Kriging procedure will be denoted \hat{R} in both settings (considering the efficiencies at $Q_{\text{high}} = 4000 \text{ m}^3/\text{h}$ or considering the interpolated values of

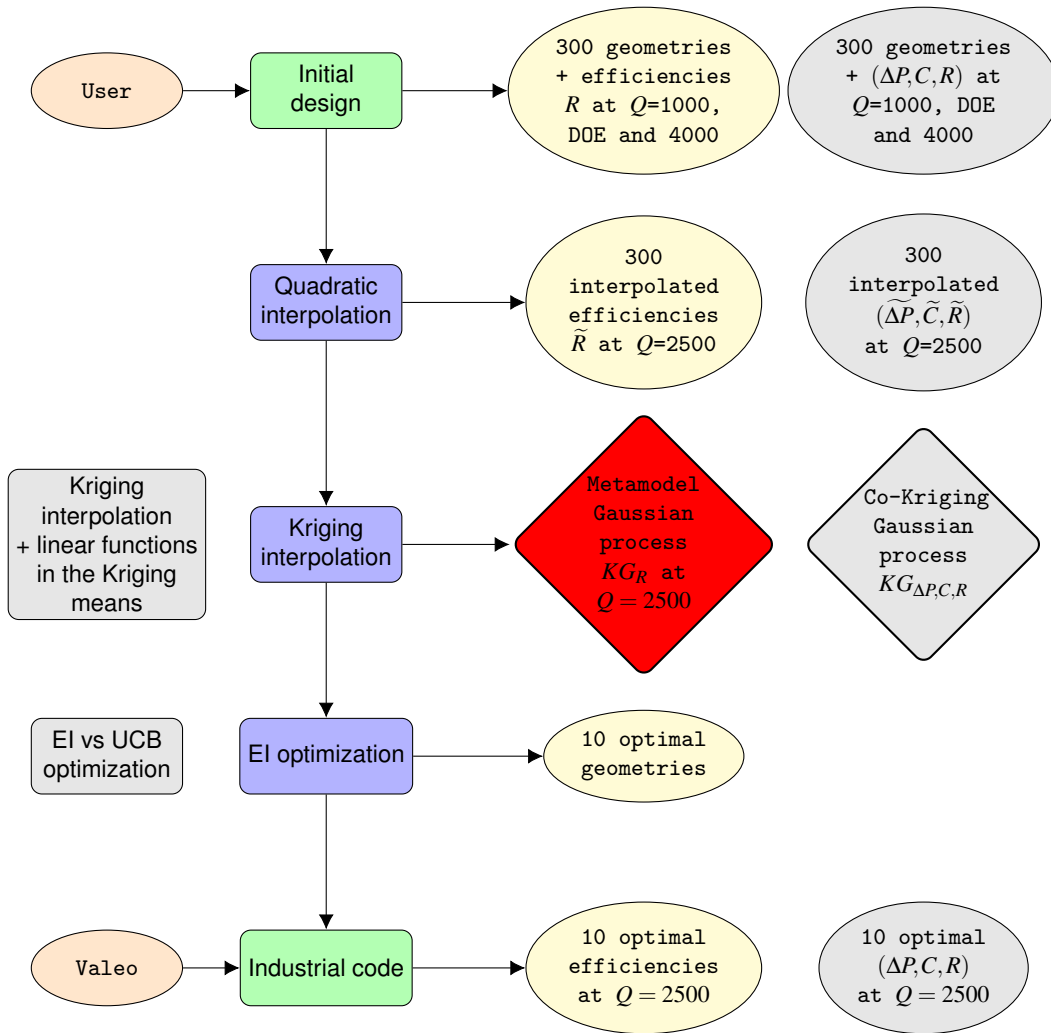


FIGURE 7. Procedure diagram when working at $Q = 2500 \text{ m}^3/\text{h}$. The gray boxes represent the directions for further research: adding linear functions in the Kriging means to improve the optimization step, comparing the upper confidence bound optimization procedure to expected improvement, and consider the whole vector $(\Delta P, C, R)$ of outputs and perform co-Kriging and multi-objective expected improvement.

the efficiencies at $Q = 2500 \text{ m}^3/\text{h}$), while the corresponding Gaussian processes will be denoted by KG_R .

5.4. Results

Performance of Kriging To measure the performance of the model, we realize a cross-validation procedure by Leave-One-Out (LOO). The LOO procedure consists in computing the prediction at a design point when the corresponding observation is removed from the learning set (and this, for all design points). See, for instance, [Cressie \(1993\)](#); [Ripley \(1981\)](#); [Bachoc \(2013\)](#) for more details on the LOO procedure. In that view, we use the function “leaveOneOut.km” of

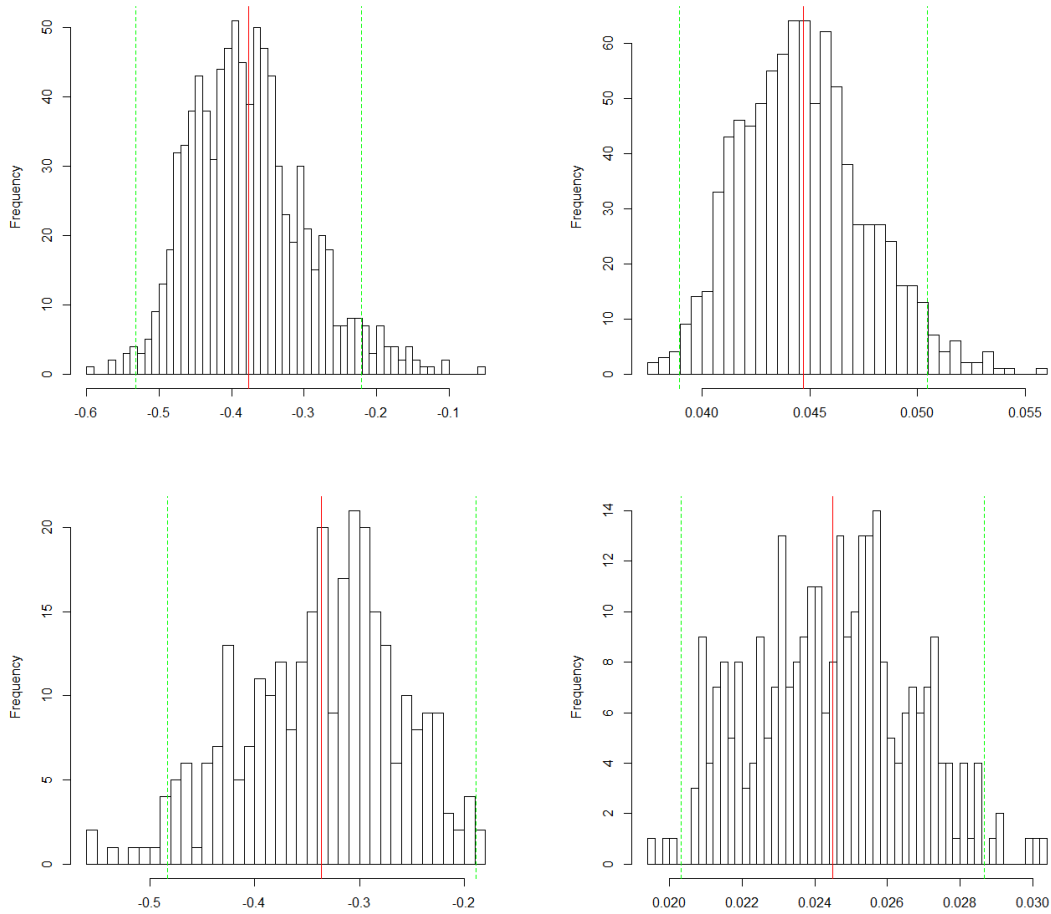


FIGURE 8. **Kriging performances.** Histograms of the mean (left) and standard deviations (right) Leave-One-Out performed on $\hat{R}(\cdot;4000)$ (up) and $\hat{R}(\cdot;2500)$ (bottom). The vertical red line denotes the mean value. The vertical green lines corresponds to the confidence intervals at 95%.

of the R package `DiceKriging` that, for any geometry i of the design of experiment, determines the associated Kriging model based on the learning sample without the i th observation point. The output of “`leaveOneOut.km`” consists in two vectors of length the number of observations N whose i th coordinates correspond to the Kriging mean and the Kriging standard deviation at the i th observation point when removing it from the learning sample.

In Figure 8, we represent the histograms of these two vectors obtained considering $\hat{R}(\cdot;4000)$ and $\hat{R}(\cdot;2500)$ together with the confidence intervals at 95%. First, no outliers are highlighted in the histograms of the conditional means (left side of Figure 8). Second, we observe that the conditional standard deviations are far from constant (right side of Figure 8), traducing the fact that the observations of the design of experiment are informative.

In Table 1, we display some classical performance criteria of the Kriging realized on the values of $\hat{R}(\cdot;4000)$ and $\hat{R}(\cdot;2500)$. Namely, we give

- the multiple R -squared error (R^2) defined by

$$R^2 = 1 - \frac{\sum_{i=1}^N (y_i - \hat{y}_i)^2}{\sum_{i=1}^N (y_i - \bar{y}_N)^2},$$

where \hat{y}_i is the prediction of the i -th data y_i and \bar{y}_N stands for the empirical mean of the data. The closest the value of one is, the best the prediction is;

- the root of the Mean Square Error (RMSE) error between the exact value and the predicted one given by

$$\text{RMSE} = \sqrt{\frac{1}{N} \sum_{i=1}^N (y_i - \hat{y}_i)^2};$$

- the Relative Maximum Absolute (RMA) error defined by

$$\text{RMA} = \max_{i=1, \dots, N} \frac{|y_i - \hat{y}_i|}{\sigma},$$

where σ stands for the standard deviation of the vector of the output values;

- the Covering Rates (CR) at 95% are given by:

$$\text{CR}(95\%) = \frac{1}{N} \sum_{i=1}^N \mathbb{1}_{\{|y_i - \hat{y}_i| \leq 1.96 \times \sigma_N(x_i)\}}$$

where $\sigma_N^2(x_i)$ stands for the Kriging variance.

Notice that the standard deviation of the efficiencies corresponding to the flow rate $Q = 4000 \text{ m}^3/h$ (resp. $Q = 2500 \text{ m}^3/h$) is 0.092 (resp. 0.079).

	Kriging on R_{4000}	Kriging on \hat{R}_{2500}
R^2	0.763	0.906
RMSE	0.045	0.024
RMA	2.281	0.888
CR(95%)	0.941	0.939

TABLE 1. *Kriging performances on both models (R_{4000} and \hat{R}_{2500})*

Both methodologies provide good results with R^2 values close to 1 and RMSE and RMA values close to 0 as expected. Surprisingly, the Kriging on the estimated efficiency at $2500 \text{ m}^3/h$ outperforms the Kriging at $4000 \text{ m}^3/h$. Thus working on an average flow rate is more efficient than working at an extreme rate of $4000 \text{ m}^3/h$ and provides more accurate results. This observation and these results validate this second procedure at $2500 \text{ m}^3/h$. Observe that the covering rates appear to be under-estimated.

Notice that adding linear functions of parameters to the Kriging mean would have been interesting and probably could have significantly improved the optimization. Such an improvement will be considered in a further study.

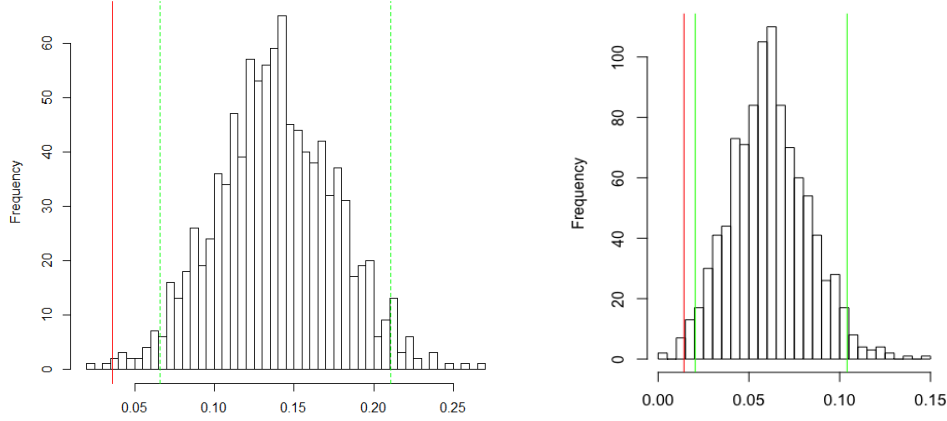


FIGURE 9. **Expected improvement performances.** Finite sample distributions of expected improvement (histograms) computed on $R(\cdot; 4000)$ (left) and $\hat{R}(\cdot; 2500)$ (right). The vertical red line denotes the a posteriori value of the EI. The vertical green lines corresponds to the confidence intervals at 95%.

Performance of expected improvement and results Now, the expected improvement algorithm gives us a batch of $n = 10$ new geometries $(g_1^{\text{new}}, \dots, g_{10}^{\text{new}})$, where $g_i^{\text{new}} \in \mathbb{R}^{14}$, for all $i = 1, \dots, 10$. Valeo engineers then compute the corresponding efficiencies. In order to have an idea of the likely improvements brought by expected improvement, we generate 1000 realizations of the efficiencies R at the 10 new geometries and $Q = 4000 \text{ m}^3/h$ conditionally to the data (the 300 efficiencies of the design of experiment) using the Kriging model. In other words, if KG_R represents the Gaussian process obtained by the Kriging procedure from the initial design of experiment, we obtain 1000 realizations of the random vector:

$$(KG_R(g_1^{\text{new}}; 4000), \dots, KG_R(g_{10}^{\text{new}}; 4000)).$$

Then, for each of the 1000 realizations, we compute the associated value of expected improvement, namely,

$$\left(\max_{j=1, \dots, 10} KG_R(g_j^{\text{new}}; 4000)[k] - \max_{j=1, \dots, \text{length}(\text{DoE})} \hat{R}(g_j; 4000) \right)^+$$

for $k = 1, \dots, 1000$, that we represent in the histograms of Figure 9. Additionally, we represent by the red line the a-posteriori value of the expected improvement obtained on the new geometries:

$$\max_{i=1, \dots, 10} \hat{R}(g_i^{\text{new}}; 4000) - \max_{j=1, \dots, \text{length}(\text{DoE})} \hat{R}(g_j; 4000)$$

We call it the true value of the expected improvement. Analogously, we consider also 1000 realizations of $(KG_R(g_1^{\text{new}}; 2500), \dots, KG_R(g_{10}^{\text{new}}; 2500))$ conditionally to the 300 estimated efficiencies at $Q = 2500 \text{ m}^3/h$.

In the left hand side of Figure 10, we represent the values of the efficiency R at $Q = 4000 \text{ m}^3/h$ for the 10 new geometries given by the expected improvement algorithm together with

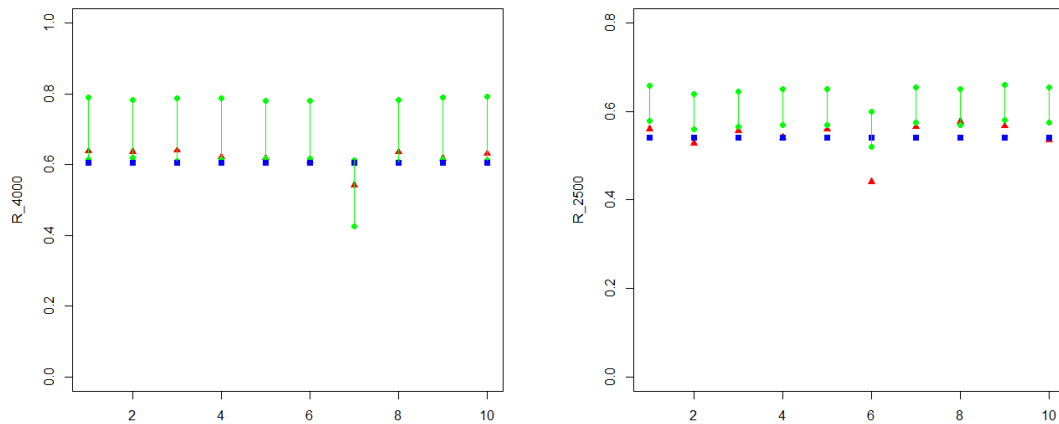


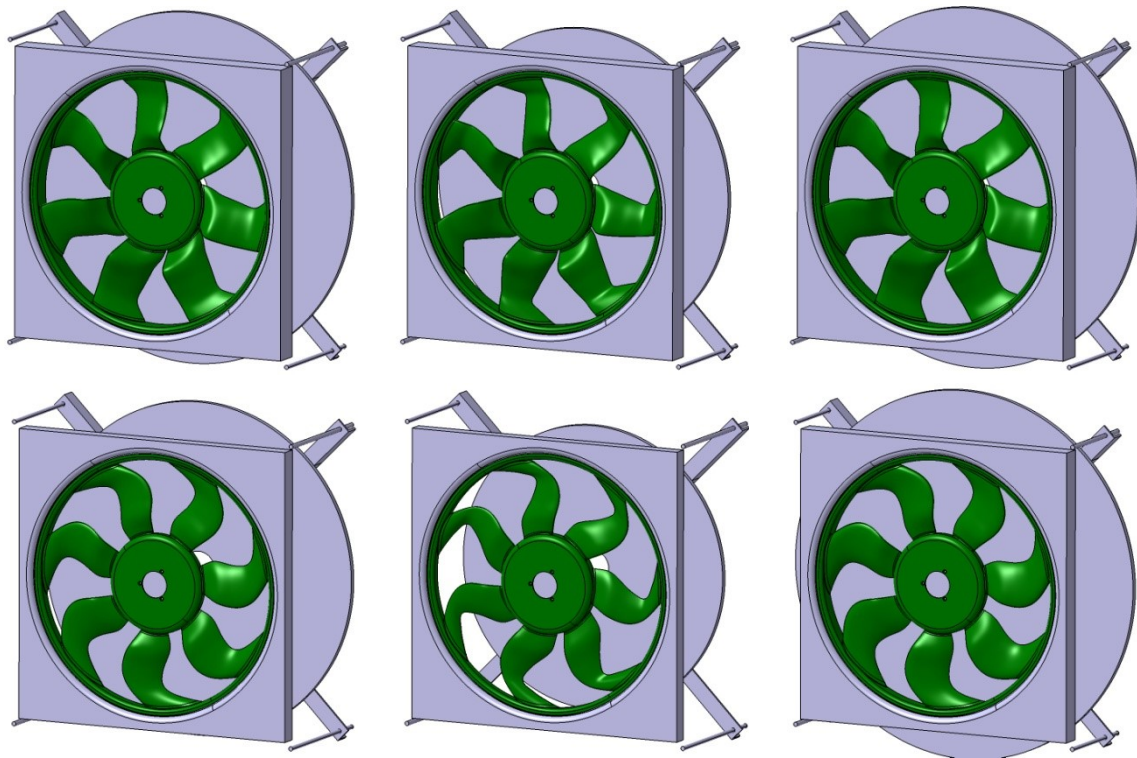
FIGURE 10. The results obtained on $\hat{R}(\cdot;4000)$ (respectively $\hat{R}(\cdot;2500)$) are represented in the left (resp. right). The red triangles give the values of the efficiency R at $Q = 4000$ for the 10 new geometries given by the expected improvement. The blue rectangles represents the current maximum. The green segments stand for the confidence intervals predicted by Kriging.

the value of the current maximum. This picture illustrates the fact that all the points correspond to exploitation (improvement of the promising regions) except the number 7 that corresponds to exploration. This fact can also be seen looking at the correlation matrix between the 10 new geometries presented in Table 2. The geometry numbered 7 is clearly uncorrelated from the others and corresponds to exploration. Moreover, notice that the confidence intervals given by Kriging are optimistic. Similarly in the right hand side of Figure 10, we represent the values of the efficiency R at $Q = 2500 \text{ m}^3/h$ for the 10 new geometries.

Although the performances of the new geometries are finally at the bottom of the confident interval, it must be emphasized that they can be considered as very good design with high efficiencies (for this kind of ventilation system). This confirms that the tool is actually able to find the most interesting areas, with various solutions. As presented in Figure 11, the targeted operating point for the optimization process determines some generic “gene” in the solutions. The searching method which is the NSGA II genetic algorithm, has obviously found for each of the optimization, either at high or a medium flow rate, two different sets of characteristics: at $4000 \text{ m}^3/h$, the optimizer has selected straight blades with two discontinuities, respectively one close to the hub, and one close to the tip (top panel in Figure 11). At $2500 \text{ m}^3/h$, the design is being modified with a smoother shape from bottom to top and a backward blade sweep (meaning that the blade is curved in a direction opposite to the rotating one) (bottom panel in Figure 11).

Skilled engineers for this type of turbomachine have confirmed the relevancy of these observations, in particular the fact that backward sweep blades are good for efficiency and that straight ones are adapted to high flow rate. However, a so wide variety of design could not be obtained with classical iterative design methods, and the benefit of the meta-modeling is clearly its efficiency in proposing numerous designs in a short time frame.

	[.1]	[.2]	[.3]	[.4]	[.5]	[.6]	[.7]	[.8]	[.9]	[.10]
[.1]	1.00000000	0.58156715	0.64818146	0.60873040	0.52468595	0.53664093	0.04283566	0.60534756	0.66981971	0.67070323
[.2]	0.58156715	1.00000000	0.53867748	0.59920321	0.59855007	0.60018872	0.03394723	0.50275974	0.58645696	0.58498154
[.3]	0.64818146	0.53867748	1.00000000	0.53393445	0.45723059	0.46774272	0.05433128	0.65886968	0.63105370	0.63127975
[.4]	0.60873040	0.59920321	0.53393445	1.00000000	0.59824959	0.60748421	0.03420089	0.47128678	0.62851412	0.63001910
[.5]	0.52468595	0.59855007	0.45723059	0.59824959	1.00000000	0.61347583	0.03068968	0.41150444	0.54010069	0.53917369
[.6]	0.53664093	0.60018872	0.46774272	0.60748421	0.61347583	1.00000000	0.03112121	0.41978435	0.55268651	0.55201157
[.7]	0.04283566	0.03394723	0.05433128	0.03420089	0.03068968	0.03112121	1.00000000	0.05476946	0.03901714	0.03961607
[.8]	0.60534756	0.50275974	0.65886968	0.47128678	0.41150444	0.41978435	0.05476946	1.00000000	0.57885056	0.57779872
[.9]	0.66981971	0.58645696	0.63105370	0.62851412	0.54010069	0.55268651	0.03901714	0.57885056	1.00000000	0.67714934
[.10]	0.67070323	0.58498154	0.63127975	0.63001910	0.53917369	0.55201157	0.03961607	0.57779872	0.67714934	1.00000000

TABLE 2. Conditional correlation matrix between the 10 new geometries considering $R(\cdot; 4000)$.FIGURE 11. Illustration of the similarities with common “genes”. Examples of optimized designs for high flow rate ($Q = 4000\text{m}^3/\text{h}$ - top panel) and medium flow rate ($Q = 2500\text{m}^3/\text{h}$ - bottom panel).

6. Conclusion

A strategy for fan optimization, based on the use of an intense campaign of simulation has been proposed and tested. The method relies on a parametric model of the fan, which defines sets of parameters that are experimented in the design of experiment process. In order to address the difficulties related to the size of the domain in the dimension 15 and to the relative seldom runs, a meta-model based on a Kriging method has been built and further used to enrich the sampling. The combination of two tips has allowed improving the model: at first, a trend based on the turbomachine theory has been implemented for the efficiency in the Kriging model. Then several batches of additional runs have been proposed thanks to a criterion that seeks for the possible maximum improvement within the variance intervals. It has been observed that despite being too much optimistic, the results proposed by the genetic algorithm that interrogates the response surface are relevant and finally all have shown good efficiencies (except one over twenty). This good achievement indicates at first that the Kriging method is able to provide the good trends and can be used for optimization, in particular if the method can be improved on one hand by the use of turbomachine rules (here for instance using the efficiency as a trend), and on the other hand by a sequential strategy that exploits the expected improvement criterion. The proposed designs for a given targeted operating point have some similarities in their shapes, showing that the optimization process selects some characteristics which are deterministic. If it is on line with previous observations from the state of the art, it is remarkable how the method has provided so efficiently a wide variety of these best performer designs. All in all, the combination of design rules, numerical simulation and mathematics in meta-modeling is perceived as a very efficient method for optimization even in average dimensions. Perspectives are even more promising for the scientific community since the CPU cost is becoming every year more affordable and the pressure for optimized turbomachines in term of efficiency is high (due to economical and ecological concerns).

Acknowledgments. The authors warmly thank the two anonymous reviewers for their helpful comments and suggestions that lead to a significant improvement of the manuscript. They also thank François Bachoc and Céline Helbert for their helpful discussions and suggestions. This work has been supported by the French National Research Agency (ANR) through PEPITO project (no ANR-14-CE23-0011).

References

- Arnaud, M. and Emery, X. (2000). *Estimation et interpolation spatiale: méthodes déterministes et méthodes géostatistiques*. Hermès.
- Auer, P., Cesa-Bianchi, N., and Fischer, P. (2002). Finite-time analysis of the multiarmed bandit problem. *Machine Learning*, 47(2):235–256.
- Bachoc, F. (2013). Cross validation and maximum likelihood estimations of hyper-parameters of Gaussian processes with model misspecification. *Comput. Statist. Data Anal.*, 66:55–69.
- Baillargeon, S. (2005). Le krigeage: revue de la théorie et application à l’interpolation spatiale de données de précipitations.
- Bect, J., Bachoc, F., and Ginsbourger, D. (2018). A supermartingale approach to Gaussian process based sequential design of experiments. working paper or preprint.
- Bryan, B. A. and Adams, J. M. (2002). Three-dimensional neurointerpolation of annual mean precipitation and temperature surfaces for china. *Geographical Analysis*, 34(2):93–111.

Soumis au Journal de la Société Française de Statistique

File: EI_SFDS_REV3.tex, compiled with jsfds, version : 2018/06/13

date: May 26, 2020

- Chevalier, C. and Ginsbourger, D. (2013). Fast computation of the multi-points expected improvement with applications in batch selection. In Nicosia, G. and Pardalos, P., editors, *Learning and Intelligent Optimization*, pages 59–69, Berlin, Heidelberg. Springer Berlin Heidelberg.
- Cressie, N. A. C. (1993). *Statistics for spatial data*. Wiley Series in Probability and Mathematical Statistics: Applied Probability and Statistics. John Wiley & Sons, Inc., New York. Revised reprint of the 1991 edition, A Wiley-Interscience Publication.
- Fletcher, R. (1987). *Practical methods of optimization*. Number vol. 1 in Wiley-Interscience publication. Wiley.
- Frazier, P. I., Powell, W. B., and Dayanik, S. (2008). A knowledge-gradient policy for sequential information collection. *SIAM J. Control Optim.*, 47(5):2410–2439.
- Gaudard, M., Karson, M., Linder, E., and Sinha, D. (1999). Bayesian spatial prediction. *Environmental and Ecological Statistics*, 6(2):147–171.
- Ginsbourger, D., Le Riche, R., and Carraro, L. (2008). A Multi-points Criterion for Deterministic Parallel Global Optimization based on Gaussian Processes. Technical report.
- Grondin, G., Kelner, V., Ferrand, P., and Moreau, S. (2005). Robust design and parametric performance study of an automotive fan blade by coupling multi-objective genetic optimization and flow parameterization. In *Proc. of the International Congress on Fluid Dynamics Applications in Ground Transportation, Lyon, France*.
- Huang, D., Allen, T. T., Notz, W. I., and Miller, R. A. (2006). Sequential kriging optimization using multiple-fidelity evaluations. *Structural and Multidisciplinary Optimization*, 32(5):369–382.
- Jin, R., Chen, W., and Sudjianto, A. (2005). An efficient algorithm for constructing optimal design of computer experiments. *J. Statist. Plann. Inference*, 134(1):268–287.
- Jones, D. R. (2001). A taxonomy of global optimization methods based on response surfaces. *Journal of global optimization*, 21(4):345–383.
- Jones, D. R., Schonlau, M., and Welch, W. J. (1998). Efficient global optimization of expensive black-box functions. *Journal of Global Optimization*, 13(4):455–492.
- Krige, D. G. (1951). A statistical approach to some basic mine valuation problems on the witwatersrand. *Journal of the Chemical, Metallurgical and Mining Society of South Africa*, 52:119–139.
- Matheron, G. (1962). *Traité de géostatistique appliquée, Tome I*, volume 14 of *Editions Technip, Paris*. Mémoires du Bureau de Recherches Géologiques et Minières.
- Matheron, G. (1963). Principles of geostatistics. *Economic Geology*, 58:1246–1266.
- Močkus, J. (1975). On bayesian methods for seeking the extremum. In Marchuk, G. I., editor, *Optimization Techniques IFIP Technical Conference Novosibirsk, July 1–7, 1974*, pages 400–404, Berlin, Heidelberg. Springer Berlin Heidelberg.
- Moreau, S., Aubert, S., Grondin, G., and Casalino, D. (2004). Geometric parametric study of a fan blade cascade using the new parametric flow solver turb’opt. In *ASME 2004 Heat Transfer/Fluids Engineering Summer Conference*, pages 1293–1298. American Society of Mechanical Engineers Digital Collection.
- Owen, A. B. (1992). Orthogonal arrays for computer experiments, integration and visualization. *Statistica Sinica*, 2(2):439–452.
- Picheny, V. (2015). Multiobjective optimization using Gaussian process emulators via stepwise uncertainty reduction. *Stat. Comput.*, 25(6):1265–1280.
- Rasmussen, C. and Williams, C. (2006). *Gaussian Processes for Machine Learning*. The MIT Press, Cambridge.
- Rice, J. A. (2006). *Mathematical statistics and data analysis*. Cengage Learning.
- Ripley, B. D. (1981). *Spatial statistics*. John Wiley & Sons, Inc., New York. Wiley Series in Probability and Mathematical Statistics.
- Roustant, O., Ginsbourger, D., and Deville, Y. (2012). Dicekriging, diceoptim: Two r packages for the analysis of computer experiments by kriging-based metamodeling and optimization. *Journal of Statistical Software, Articles*, 51(1):1–55.
- Santner, T. J., Williams, B. J., and Notz, W. (2003). *The design and analysis of computer experiments*, volume 1. Springer.
- Sasena, M. J., Papalambros, P., and Goovaerts, P. (2002). Exploration of metamodeling sampling criteria for constrained global optimization. *Engineering optimization*, 34(3):263–278.
- Schonlau, M. (1997). Computer experiments and global optimization.
- Scott, W., Frazier, P., and Powell, W. (2011). The correlated knowledge gradient for simulation optimization of continuous parameters using Gaussian process regression. *SIAM J. Optim.*, 21(3):996–1026.
- Srinivas, N., Krause, A., Kakade, S. M., and Seeger, M. W. (2012). Information-theoretic regret bounds for gaussian

- process optimization in the bandit setting. *IEEE Transactions on Information Theory*, 58(5):3250–3265.
- Stein, M. (1999). *Interpolation of Spatial Data: Some Theory for Kriging*. Springer, New York.
- Vazquez, E. and Bect, J. (2010). Convergence properties of the expected improvement algorithm with fixed mean and covariance functions. *J. Statist. Plann. Inference*, 140(11):3088–3095.